Base Isolation and Supplemental Damping Systems for Seismic Protection of Wood Structures: Literature Review

Michael D. Symans,[a) M.EERI], William F. Cofer,[b)] and Kenneth J. Fridley[c)]

This paper provides a literature review on the application of base isolation and supplemental damping systems for seismic protection of wood structures. The review reveals that both elastomeric bearings and sliding bearings have been considered for implementation within base isolation systems of wood-framed buildings. In addition, friction dampers, viscoelastic dampers, hysteretic dampers, and fluid viscous dampers have been considered for implementation within the framing of wood buildings. Although there are a number of impediments to the widespread implementation of such advanced seismic protection systems, the reviewed literature clearly demonstrates that advanced seismic protection systems offer promise for enabling light-framed wood structures to resist major earthquakes with minimal damage.
[DOI: 10.1193/1.1503342]

INTRODUCTION

Light-framed wood construction has generally been regarded as performing well during moderate to strong earthquakes. Such performance is primarily due to the low mass of light-framed construction combined with its ability to deform inelastically without inducing collapse of the structure. Although light-framed wood structures typically do not collapse during moderate to strong earthquakes, the inelastic response is generally associated with significant structural and nonstructural damage that may be very costly to repair. As an example of the magnitude of the damage to light-framed wood buildings during a moderate earthquake, consider the 1994 Northridge Earthquake (Moment Magnitude = 6.8) in which it has been estimated that there was in excess of $20 billion worth of damage to such structures (Kircher et al. 1997). Obviously, the 1994 Northridge Earthquake provides clear evidence that conventional light-framed wood buildings are prone to significant damage when subjected to strong earthquake ground motions.

One approach to mitigating the effects of strong earthquakes on light-framed wood buildings is to incorporate an advanced seismic protection system within the building. For example, the response of the building can be de-coupled from the earthquake ground

[a)]Associate Professor, Dept. of Civil and Env. Engineering, Rensselaer Polytechnic Institute, 4044 Jonsson Engineering Center, 110 Eighth St, Troy, NY 12180-3590. symans@rpi.edu
[b)]Associate Professor, Dept. of Civil and Env. Engineering, Washington State University, Pullman, WA 99164-2910. cofer@wsu.edu
[c)]Associate Dean, Research and Information Technology, Howard R. Hughes College of Engineering, University of Nevada, Las Vegas; 4505 Maryland Parkway; Las Vegas, NV 89154. fridley@egr.unlv.edu

Earthquake Spectra, Volume 18, No. 3, pages 549–572, August 2002;

motion by introducing a flexible interface (i.e., a base isolation system) between the foundation and superstructure. The isolation system either shifts the fundamental period of the structure to a large value or limits the amount of force that can transferred to the structure such that interstory drifts (related to both structural and nonstructural damage) and floor and roof accelerations (related to contents damage) are reduced significantly. Alternatively, the seismic response of a building can be reduced by introducing a supplemental damping system within the framing of the building. The argument has been made that wood-framed buildings would not benefit from a supplemental damping system since the effective damping ratio of such structures is quite high (on the order of 7 to 15%). However, one must recognize that such levels of effective damping are the result of appreciable inelastic behavior associated with structural damage. A supplemental damping system would dissipate a portion of the seismic input energy, thereby reducing the amount of energy dissipated via inelastic behavior within the structural framing.

The number of applications of advanced seismic protection systems within buildings has been steadily growing within approximately the past ten years. Nearly all of these applications have been within either steel or concrete structures (e.g., see Soong and Constantinou 1995). The two most common types of base isolation systems utilize either rubber bearings or sliding bearings between the foundation and superstructure. In contrast, there are a wide variety of supplemental damping systems available for implementation in buildings (Constantinou and Symans 1993a, Constantinou et al. 1998). However, the most rapid growth in the application of supplemental damping systems to buildings has occurred for fluid viscous dampers. Since the first experimental studies on a scale-model steel building frame in 1993 (Constantinou and Symans 1993b), the number of implementations of fluid viscous dampers within major bridge and building structures has grown to 68 with installation pending in 16 additional structures. Although there are many factors that have contributed to this rapid growth, one of the primary reasons is the high energy dissipation density of fluid viscous dampers (i.e., fluid viscous dampers are capable of dissipating a large amount of energy relative to their size).

The number of studies that have been conducted on the application of advanced systems for seismic protection of wood frame structures is relatively small. This may be partially due to a number of impediments to the implementation of base isolation and supplemental damping systems in wood-framed structures. For example, the application of a base isolation system to a wood-framed structure requires the introduction of a stiff diaphragm at the first floor, the introduction of flexible utility connections (e.g., gas, electric, telecommunications, etc.), educating the builder and/or building owner on the operation and expected performance of the protection system, and convincing the builder and/or the building owner of the value of the protection system relative to its cost. In addition, applications to new construction would require changing the typical construction schedule and standard practices of construction. For supplemental damping systems, some of the same issues apply and, in addition, a modified framing arrangement would be required. In spite of the aforementioned impediments, it is evident from the literature reviewed in this paper, a summary of which appears in Table 1, that advanced seismic protection systems offer promise for improving the seismic response of light-framed wood construction.

Table 1. Summary of studies conducted on advanced seismic protection systems for wood-framed structures

Authors	Year	Topic	Type of Study
Base Isolation Systems			
Delfosse	1982	Elastomeric bearings applied to 1-story residential building	Analysis
Reed and Kircher	1986	Elastomeric bearings and sliding bearings applied to 5- story building	Analysis
Sakamoto et al.	1990	Elastomeric bearings applied to 2-story residential building	- Analysis - Experimental - Implementation
Pall and Pall	1991	Flat sliding bearings applied to 2-story residential building	- Analysis - Implementation
Zayas and Low	1997	Friction pendulum system bearings applied to 4-story apartment building	- Analysis - Implementation
Supplemental Damping Systems			
Authors	**Year**	**Topic**	**Type of Study**
Filiatrault	1990	Friction dampers applied to shear wall	Analysis
Dinehart and Shenton; Dinehart et al.	1998 1999	Viscoelastic dampers applied to shear wall	Experimental
Higgins	2001	Hysteretic dampers applied to shear wall	- Analysis - Experimental
Symans et al.	2002	Fluid viscous dampers applied to shear wall	Analysis

BASE ISOLATION SYSTEMS FOR WOOD-FRAMED BUILDINGS

DELFOSSE (1982)

Delfosse (1982) discusses issues associated with the application of base isolation systems to light structures. It is noted that the design of an elastomeric bearing isolation system for light structures may be problematic due to the low mass of such structures and the requirement for a stiff wood floor or a concrete slab spanning between the isolators. As a rough approximation, assume that a light structure supported on an isolation system behaves as a rigid body having mass *m*. In this case, the natural period of the base-isolated structure is given by

$$T=2\pi\sqrt{\frac{m}{k}} \tag{1}$$

where *k* is the lateral stiffness of the isolation system (assumed to behave elastically). Assuming the desired range of natural periods of base-isolated structures is from 1.5 to 4 seconds, the corresponding range of stiffness to mass ratios is:

$$2.5 < \frac{k}{m} < 17.5 \tag{2}$$

Thus, for structures with low mass (such as light-framed wood construction), the stiffness must be low enough to provide stiffness to mass ratios of less than about 20. Note that this relation between mass and stiffness is applicable to isolated structures in which the isolation system can be characterized by an elastic component that provides a restoring force. For isolation systems employing elastomeric bearings, the requirement for low stiffness tends to result in slender elastomeric bearings that may be prone to excessive shear strain and buckling. In spite of these apparent difficulties, Delfosse (1982) demonstrates, through an example design, that it is feasible to utilize an elastomeric base isolation system for a single-story wood-framed house. The example design is a one-story wood-framed house that is rectangular in plan (12 m$\times$10 m) with a seismic mass of 29,770 kg. The elastomeric base isolation system is designed to protect the structure when it is subjected to a 5%-damped design spectrum corresponding to an earthquake having a Richter magnitude of 8 and a peak ground acceleration of 0.5 g. The design is intended to limit the spectral acceleration to 0.33 g so as to produce essentially elastic behavior of the structure and thus ensuring the life-safety of the occupants and protecting the building contents. The design results in a natural period of 1.4 sec for the base-isolated building. Note that no information is provided on the natural period of the fixed-base building (i.e., the building with a conventional foundation).

REED AND KIRCHER (1986)

Reed and Kircher (1986) discuss a seismic retrofit study on a five-story wood-frame building using two different isolation system configurations; one with elastomeric bearings and the other with flat sliding bearings. The building, constructed in 1886, is part of the Naval Postgraduate School in Monterey, California, and has both historical and architectural significance to the U.S. Navy. For both isolation system configurations, a horizontal steel truss system was designed to stiffen the first floor so as to achieve rigid diaphragm action immediately above the isolation level. In addition, a vertical truss system was designed to transfer loads between the isolation system and the wood-framed superstructure. Furthermore, two restraint systems were developed; one to maintain rigidity under wind loading and the other to prevent building collapse under extreme earthquake loading. The isolation systems were designed to limit the forces transferred into the structure to 7% of the structure weight such that the structure remains essentially elastic under the design earthquake corresponding to a peak ground acceleration of 0.27 g. Thus, the wood framing above the first floor required no modification, which is often an important consideration for the retrofit of structures having historical value. The fundamental natural period of the base-isolated structure that utilizes elastomeric bearings is 2.3 seconds. The natural period of the fixed-base building was not provided. The structure with the sliding isolation system configuration is characterized by a sliding coefficient of friction of about 1%. Numerical analyses of the existing and retrofitted (i.e., base-isolated) structures subjected to three earthquake time-histories, scaled to match the peak ground acceleration of the design spectrum, produced peak base shear

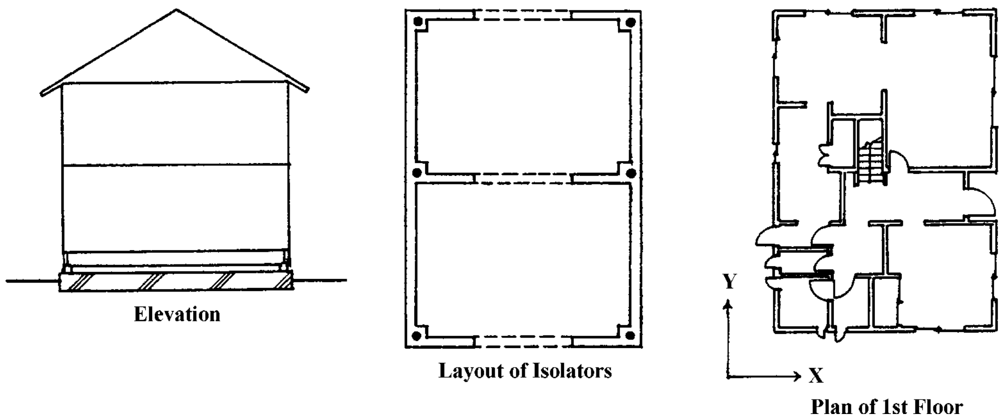

Figure 1. Plan and elevation views of two-story light-framed wood building with an elastomeric base isolation system. (Adapted from Sakamoto et al., 1990.)

response reductions ranging from 74% to 98%. Thus, the isolation systems appear to be very effective in terms of limiting the force transferred into the wood-framed superstructure.

SAKAMOTO et al. (1990)

Sakamoto et al. (1990) present an experimental and analytical study of a two-story light-framed wood building supported on a base isolation system. The building was constructed at the University of Tokyo for in-field (not laboratory) experimental testing purposes. Plan and elevation views of the structure are shown in Figure 1. The footprint of the building is 7.28 m$\times$10.92 m and the total weight is 549 kN. The base isolation system consists of six laminated elastomeric bearings located along the perimeter of the foundation (see Figure 1). Note that, although not explained by Sakamoto et al. (1990), it is apparent from Figure 1 that the isolation bearings would need to be tied together via a stiff first floor diaphragm. Three different types of bearings were used in the experimental testing; namely, high damping rubber bearings, multi-stage rubber bearings, and lead-rubber bearings (see Figure 2). The hysteretic behavior of the isolation system for the building with multi-stage rubber bearings (Type B: Center bearing of Figure 2) is

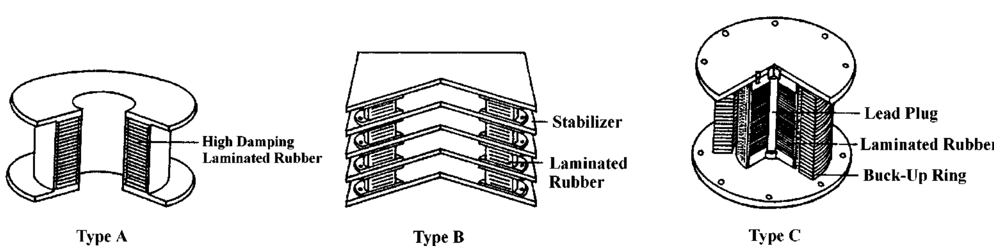

Figure 2. Configuration of elastomeric bearings used in experimental wood building. (Adapted from Sakamoto et al., 1990.)

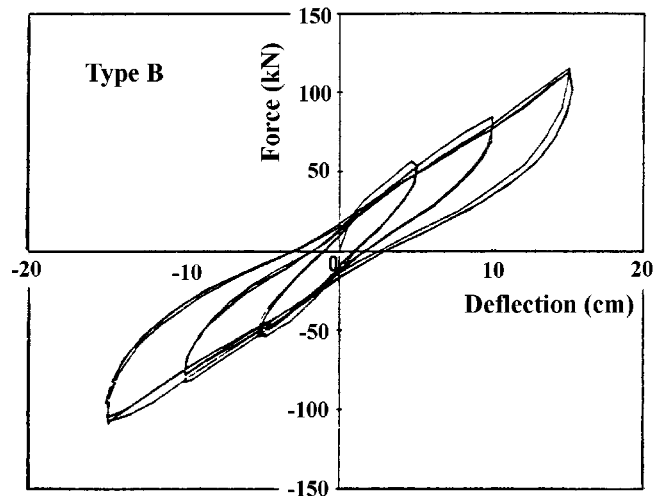

Figure 3. Hysteretic behavior of isolation system for building with multi-stage elastomeric isolation bearings. (Adapted from Sakamoto et al., 1990.)

shown in Figure 3. All of the bearing types were designed to provide a fundamental natural frequency of 0.5 Hz (natural period of 2.0 sec) at a displacement amplitude of 15 cm, an equivalent viscous damping ratio of 15%, and an allowable deformation of 25 cm. The natural period of the fixed-base structure was not provided. For bearing displacements larger than 15 cm, a fail-safe support mechanism is activated in which the bottom of the first floor contacts the top of a rigid pedestal. Additional motion of the isolation system is impeded by sliding friction between the first floor and pedestal.

Free vibration tests of the isolated building in the direction of the short plan dimension revealed two dominant frequencies at about 0.8 Hz (first mode) and 8.5 Hz (second mode). The motion of the building with the multi-stage rubber bearings was also recorded during three different earthquakes. The strongest ground motion recorded and associated acceleration response of the building in the direction of the short plan dimension (i.e., the X-direction of Figure 1) are shown in Figure 4. Note that the peak ground acceleration at the building site was 0.108g. The effectiveness of the isolation system is demonstrated by the reduction of acceleration (approximately 70%) transmitted from the ground level to the first floor. The dominant frequencies in the recorded acceleration response occurred at about 2.1 Hz and 9.7 Hz. The difference in fundamental frequencies for the free vibration response (0.8 Hz) and earthquake loading response (2.1 Hz) is attributed to the nonlinear behavior of the rubber bearings. The maximum displacement in the free vibration and earthquake loading tests was 15 cm and 0.1 cm, respectively. Since the effective stiffness of the bearings reduces with increasing displacement (see Figure 3), it is expected that the free vibration response (larger amplitude, lower stiffness) would be dominated by lower frequencies of motion. Finally, numerical simulations were performed for the building in a fixed-base and base-isolated configuration and subjected to the same earthquake as that described above. The numerical simulations were performed using a linear model of the building and isolation system in which ef-

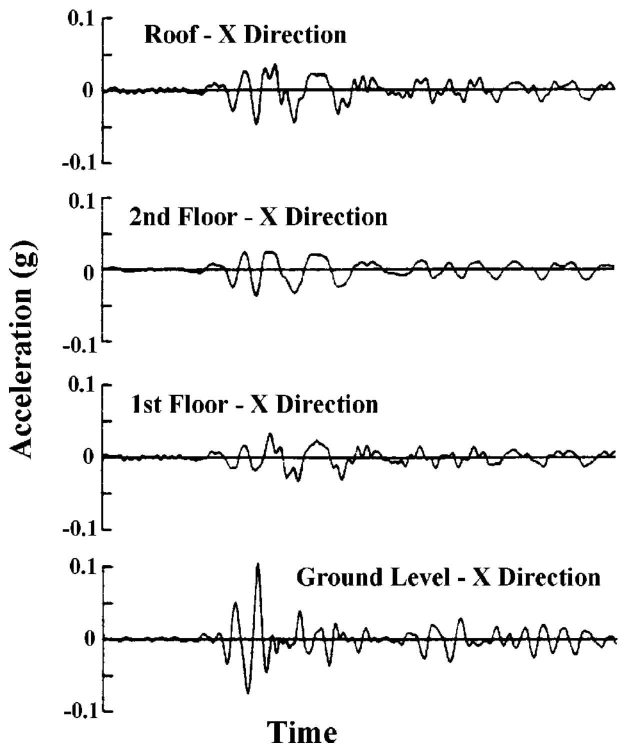

Figure 4. Acceleration response of wood building subjected to earthquake ground motion. (Adapted from Sakamoto et al., 1990.)

fective system properties were determined by matching simulation results with the recorded seismic response of the building. The simulations indicated that the peak acceleration at the roof of the fixed-base structure would be about ten times as large as for the base-isolated structure.

PALL AND PALL (1991)

In 1988, a base isolation system was implemented within a two-story light-framed wood house in Montreal, Canada (Pall and Pall 1991). A photograph of the house is shown in Figure 5 and a plan view showing the location of the isolation bearings is shown in Figure 6. The house has two stories above grade and a basement below grade. The basement walls are reinforced concrete and the superstructure consists of light-framed wood construction with brick veneer. The isolation bearings used in this application are flat sliding bearings. A total of 15 bearings were installed along the perimeter of the basement wall. Note that the bearings were flat in the center with ramped surfaces along the edges (see Section 1-1 of Figure 6). The ramped surfaces provide increasing resistance at large displacements. The isolation gap is protected from the elements via flashing on the outside of the gap (see Section 1-1 of Figure 6). The coefficient of friction associated with the sliding interface of the bearings is 0.2. The coefficient of friction determines the maximum lateral force that can be transferred to the superstructure.

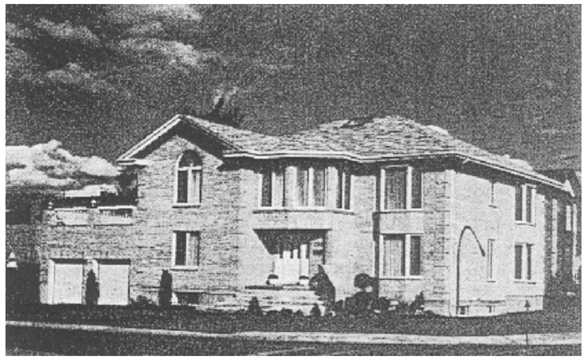

Figure 5. Photograph of wood-framed house with sliding base isolation system. (From Pall and Pall 1991, © University of Toronto Press. Reproduced with permission.)

In addition, the sliding friction dissipates energy as the bearing is cycled. Note that the natural period of a structure supported on flat sliding bearings is displacement-dependent and thus resonant response is not a concern.

Numerical analyses of the house in a fixed-base and base-isolated configuration were performed with earthquake ground motion represented by an artificial earthquake record. The earthquake record was developed to be consistent with the design response

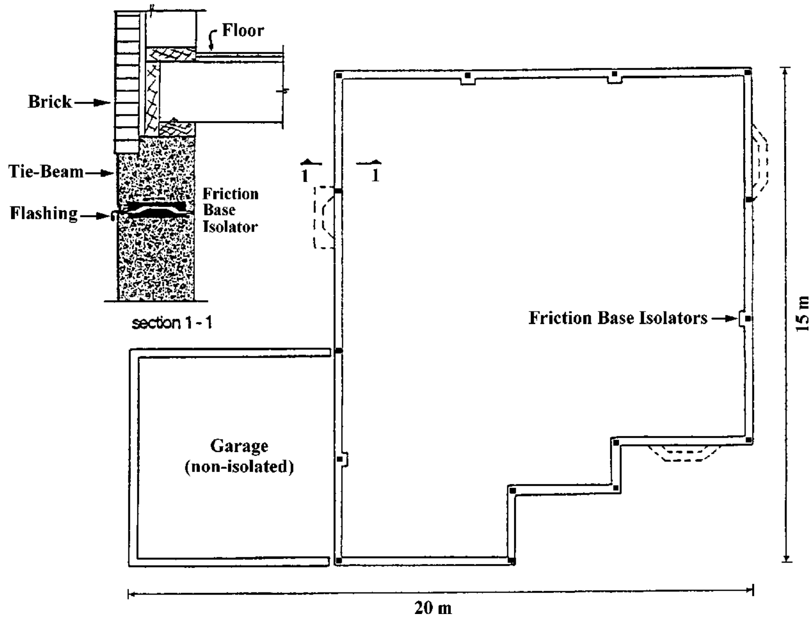

Figure 6. Plan view of wood-framed house showing location of sliding isolation bearings. (Adapted from Pall and Pall 1991, © University of Toronto Press. Reproduced with permission.)

Figure 7. Photograph of four-story wood-framed apartment building seismically retrofitted with a sliding isolation system. (From Zayas and Low 1997, © Forest Products Society. Reproduced with permission.)

spectrum of the National Building Code of Canada. The results of the analyses show that the acceleration at the top of the structure is reduced by about 42% for the design peak ground acceleration of 0.18 g. This reduction in acceleration response is accompanied by a peak bearing displacement of 3 mm and a permanent displacement of 1.5 mm. Furthermore, as the peak ground acceleration increases, the effectiveness of the isolation system increases (i.e., the reductions in response acceleration are larger). Interestingly, the improved seismic performance did not reduce the cost of materials for construction of the house since standard size materials were used. Furthermore, the cost of the 15 isolators was $8,000. However, Pall and Pall (1991) suggest that the relatively low cost of friction base isolation bearings will result in widespread application of such bearings in low-rise construction including wood-framed houses.

ZAYAS AND LOW (1997)

The implementation of sliding bearings in a four-story wood-framed apartment building in San Francisco, California, is discussed by Zayas and Low (1997). The building was severely damaged during the 1989 Loma Prieta earthquake and was retrofitted using sliding friction pendulum system (FPS) bearings. The four-story structure has a garage at the first story with apartments in the top three stories (see Figure 7). The damage to the first story during the Loma Prieta earthquake was so severe that the entire first-story wood framing was replaced with a steel moment-resisting frame. The design of the frame was such that the structure exhibited essentially elastic behavior for a design earthquake with a peak ground acceleration of 0.21 g. The sliding bearings were installed under the base plates of each column of the steel frame (see Figure 8). Thus, the gravity loads of the structure are no longer transferred to the foundation over continuous sill plates but rather are transferred at the discrete locations of the bearings. The FPS bearings have a curved sliding surface with a constant radius of curvature (i.e., the sliding surface is circular in two dimensions and spherical in three dimensions) (see Figure 9). The motion of the structure when supported on the bearings is similar to that of a simple pendulum. The curved surface results in both energy dissipation due to sliding

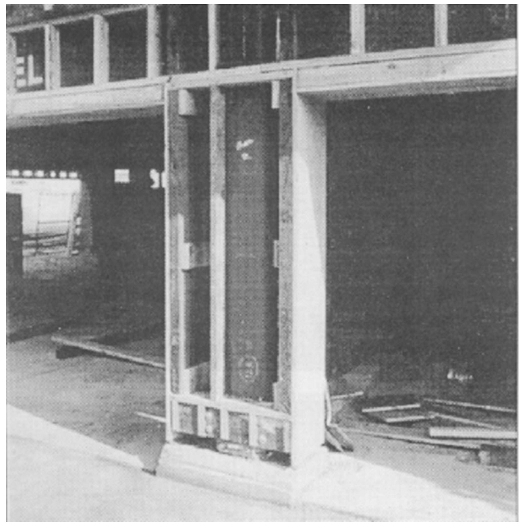

Figure 8. Close-up view of column showing isolation bearing installed below base plate. (From Zayas and Low 1997, © Forest Products Society. Reproduced with permission.)

friction and energy storage due to the rising of the supported weight along the curved surface. In contrast to the behavior of structures supported on flat sliding bearings, structures supported on curved bearings exhibit a natural period that can be determined by analogy to the natural period of a simple pendulum:

$$T=2\pi\sqrt{\frac{R}{g}} \tag{3}$$

where R is the radius of curvature of the bearings, g is the acceleration due to gravity, and it has been assumed that the superstructure behaves as a rigid body. Interestingly, the natural period is independent of the weight supported by the bearings. Thus, the low mass of light-framed wood structures does not pose a problem for an isolation system that utilizes FPS bearings (recall that the potential for buckling of slender elastomeric bearings is due to the low mass supported by the bearing). The design of the bearings was based on a nonlinear, three-dimensional dynamic analysis using design earthquakes

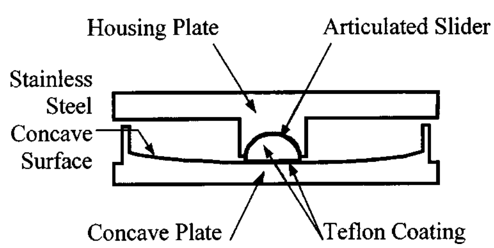

Figure 9. Cross section of friction pendulum system bearing.

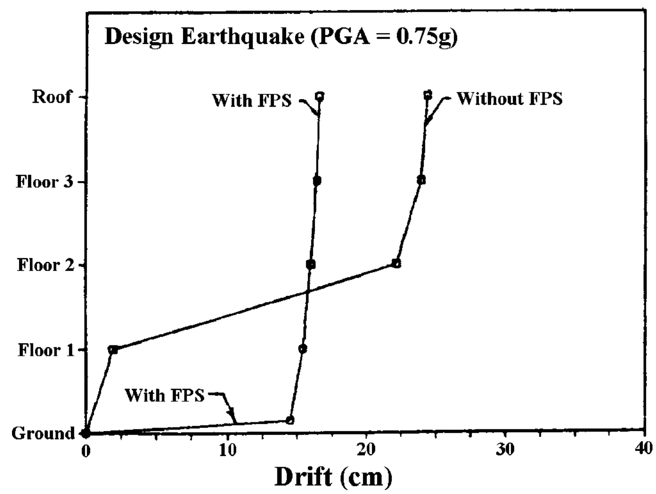

Figure 10. Relative displacement response profiles for fixed-base and base-isolated configurations. (Adapted from Zayas and Low 1997, © Forest Products Society. Reproduced with permission.)

corresponding to the site-specific spectra for a magnitude 7 earthquake on the San Andreas Fault located seven miles from the building site. The final design of the bearings resulted in a natural period of 2 seconds, a coefficient of friction of 10%, a displacement capacity of ± 19 cm, and a required seismic gap of 28 cm. Note that no information was provided on the natural period of the fixed-base structure.

The performance of the base-isolated structure was evaluated via nonlinear time-history analysis. The results for input being a design-level earthquake with peak ground acceleration of 0.75g is presented here. Note that the design earthquake was considered to be representative of a site-specific spectrum corresponding to a magnitude 7 earthquake on the San Andreas Fault (approximately 11.3 km from the site). Relative displacement response profiles are compared in Figure 10 for two cases: 1) fixed-base configuration (but with first story strengthened by steel moment-resisting frame) and 2) isolated configuration. As expected, the displacement response of the isolated building is concentrated at the isolation level with very little interstory drift response in the superstructure. In contrast, the non-isolated building experiences significant interstory drift that is concentrated in the second story. The effect of the isolation system is to reduce the peak interstory drift by about 95%. The isolated building remains entirely elastic while the non-isolated building experiences a ductility demand of 38.4 for the second story. Zayas and Low (1997) suggest that such a high ductility demand is beyond the reasonable capacity of the wood-stucco frame and thus there is a significant risk of collapse of the non-isolated building. In summary, the numerical analyses demonstrate that the isolated structure would respond elastically if subjected to a magnitude 7 earthquake on the nearby San Andreas Fault. Finally, it is noted that retrofitting the building using a seismic isolation system was cost effective in that its use avoided the need to add shear

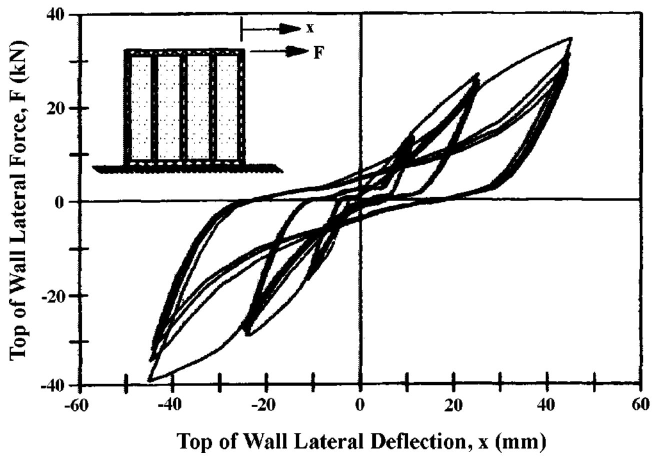

Figure 11. Hysteretic behavior of conventional light-framed wood shear wall. (Adapted from Filiatrault 1990, © John Wiley & Sons Limited. Reproduced with permission.)

walls over the height of the structure and to remove and replace ornate finish materials having architectural significance. The cost of adding the FPS bearings and the seismic gap details was \$35.50 per m^2.

SUPPLEMENTAL DAMPING SYSTEMS FOR WOOD-FRAMED BUILDINGS

FILIATRAULT (1990)

The seismic response of friction-damped timber shear walls has been studied by Filiatrault (1990). The cyclic lateral force-displacement relation for conventional light-framed shear walls exhibits both a progressive loss of stiffness and pinching of the hysteresis loops (see Figure 11). Such behavior is a direct result of damage to the shear wall. Note that, due to the pinching of the hysteresis loops, the shear wall must experience large deformations in order to dissipate the seismic input energy. Filiatrault (1990) proposed the concept of installing supplemental energy dissipation elements at the four corners of a shear wall (see Figure 12). The elements are friction dampers that absorb a significant portion of the seismic input energy, reducing the amount of energy that needs to be dissipated by the framing via inelastic behavior. The friction dampers consist of a slotted slip joint that dissipates energy via friction as the two sides of the joint slide with respect to each other. Sliding motion of the slip joint is induced by deformation of the four corners of the shear wall. Thus, the wood framing of the shear wall must deform to activate the friction dampers. However, since the friction dampers absorb a portion of the seismic energy input, the energy dissipation demand on the framing will be reduced. Note that the triangular configuration of the friction damper (see Figure 12) is beneficial in maintaining the integrity of the wood-framed corners of the shear wall. The stability of the mechanical properties of the friction damper are demonstrated in Figure 13, which shows the repeatability of the force-displacement relation for a single damper subjected to 50 cycles of sinusoidal motion at a frequency of 0.2 Hz and an amplitude of ± 1.52 cm.

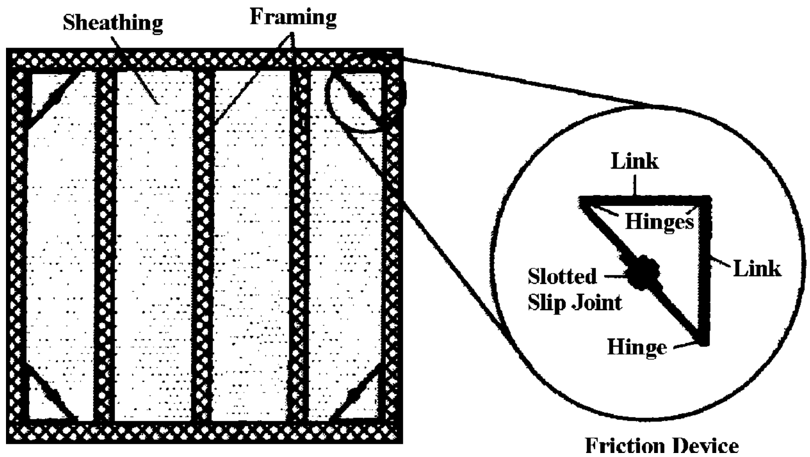

Figure 12. Shear wall with friction dampers located at four corners of framing. (From Filiatrault 1990, © John Wiley & Sons Ltd. Reproduced with permission.)

Numerical analysis of a friction-damped shear wall (2.4 m×2.4 m) was performed using nonlinear models for the shear wall and the friction dampers. The shear wall consisted of 38×89 mm spruce-pine-fir stud framing with center-to-center spacing of 600 mm and 9 mm thick plywood sheathing. The model of the shear wall accounts for both stiffness degradation and pinching of the hysteresis loops. Experimental test data obtained from shaking table tests of the shear wall without friction dampers (Dolan 1989) demonstrated the suitability of the analytical model of the shear wall. A comparison of the hysteretic behavior of the shear wall with and without the supplemental friction dampers and subjected to the El Centro record (component NS) of the 1940 Imperial

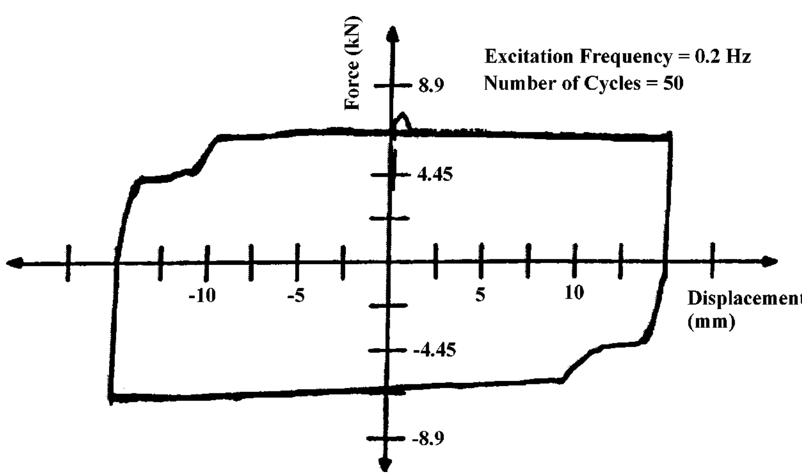

Figure 13. Hysteretic response of friction damper for steady-state sinusoidal motion. (Adapted from Filiatrault 1990, © John Wiley & Sons Ltd. Reproduced with permission.)

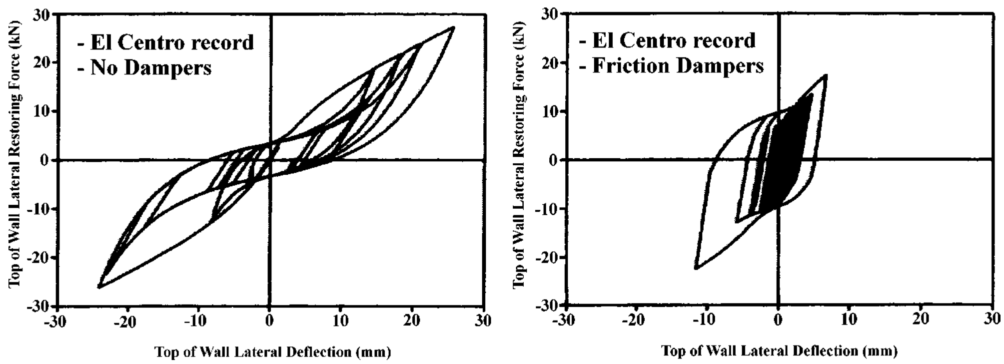

Figure 14. Effect of friction dampers on the hysteretic behavior of a wood-framed shear wall (Adapted from Filiatrault 1990, © John Wiley & Sons Ltd. Reproduced with permission.)

Valley earthquake is shown in Figure 14. The friction dampers improve the seismic performance by reducing the peak force and displacement at the top of the wall and essentially eliminating the pinching of the hysteresis loops. The effectiveness of the friction dampers is also demonstrated in the energy time histories shown in Figure 15. There is a marked reduction in the hysteretic energy dissipation demand on the shear wall. Furthermore at the end of the earthquake, approximately 60% of the input energy is dissipated by the friction dampers.

DINEHART AND SHENTON (1998); DINEHART et al. (1999)

The dynamic behavior of light-framed wood shear walls with viscoelastic dampers was experimentally evaluated by Dinehart and Shenton (1998) and Dinehart et al. (1999). The experimental tests were conducted on 2.44 m×2.44 m (8 ft×8 ft) shear walls framed with 38 mm×89 mm (2 in.×4 in., nominal) interior studs spaced at 40.6

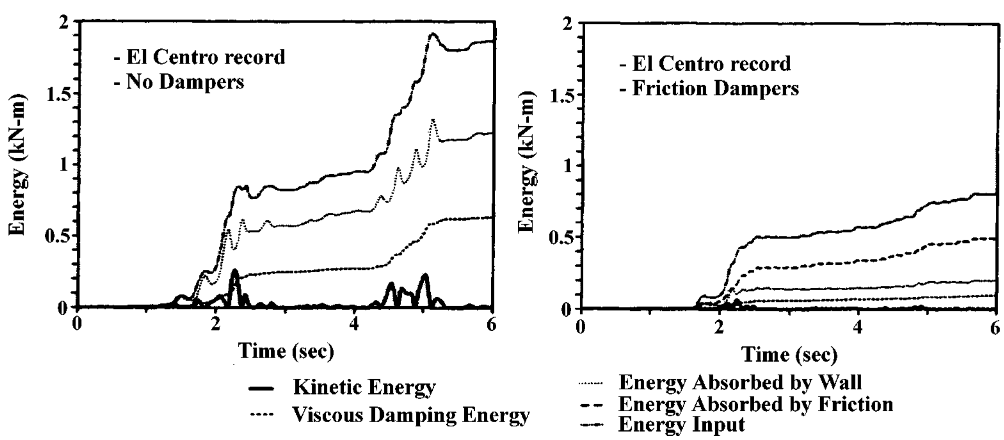

Figure 15. Effect of friction dampers on the energy distribution within a wood-framed shear wall (adapted from Filiatrault 1990, © John Wiley & Sons Ltd. Reproduced with permission).

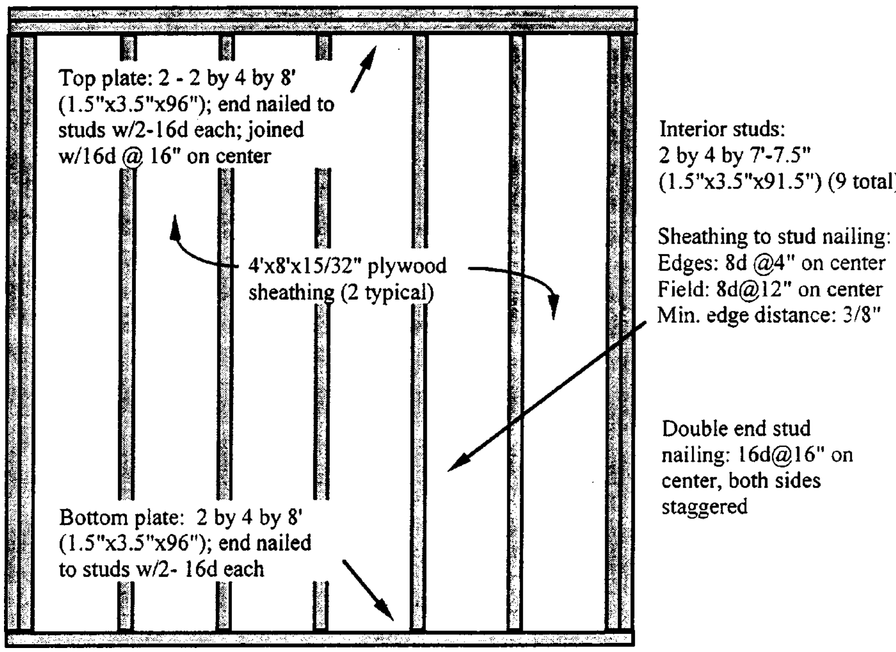

Figure 16. Configuration of conventional light-framed wood shear wall. (From Dinehart et al. 1999, © Earthquake Engineering Research Institute. Reproduced with permission.)

cm (16 in.) on center. Two 11.9 mm (15/32 in.) thick plywood sheets were used as sheathing panels (see Figure 16). Four different damper configurations were investigated (see Figure 17 and 18). In each configuration, the viscoelastic damper dissipates energy via shearing action of a viscoelastic rubber-like material. The shearing action is induced by relative motion between the two ends of the damper at their points of attachment to the shear wall. Thus, the shear wall must deform for the viscoelastic dampers to dissipate energy. In addition to the corner damper configuration shown in Figure 17a where the dampers are located in the top corners, a separate configuration with the dampers located in the bottom corners was investigated.

The shear walls were supported at the bottom plate and a prescribed lateral displacement time history was imposed at the top plate. The prescribed displacement time history consisted of 72 cycles of varying displacement amplitude (specifically, the sequential phased displacement test protocol was used.) The hysteretic behavior for the conventional wall (no dampers) and the wall with two different viscoelastic damper configurations (sheathing-to-stud and diagonal bracing) is shown in Figure 19. Due to the viscoelastic nature of the dampers, both the effective stiffness and energy dissipation increased by adding the dampers to the wall. However, as a result of utilizing a prescribed displacement time history, the hysteresis loops are not dramatically different for the conventional and viscoelastically damped walls. Although the hysteresis loops are not very different, the cumulative energy dissipated by the conventional and viscoelastically damped walls is significantly different (e.g., the cumulative energy dissipated up to the

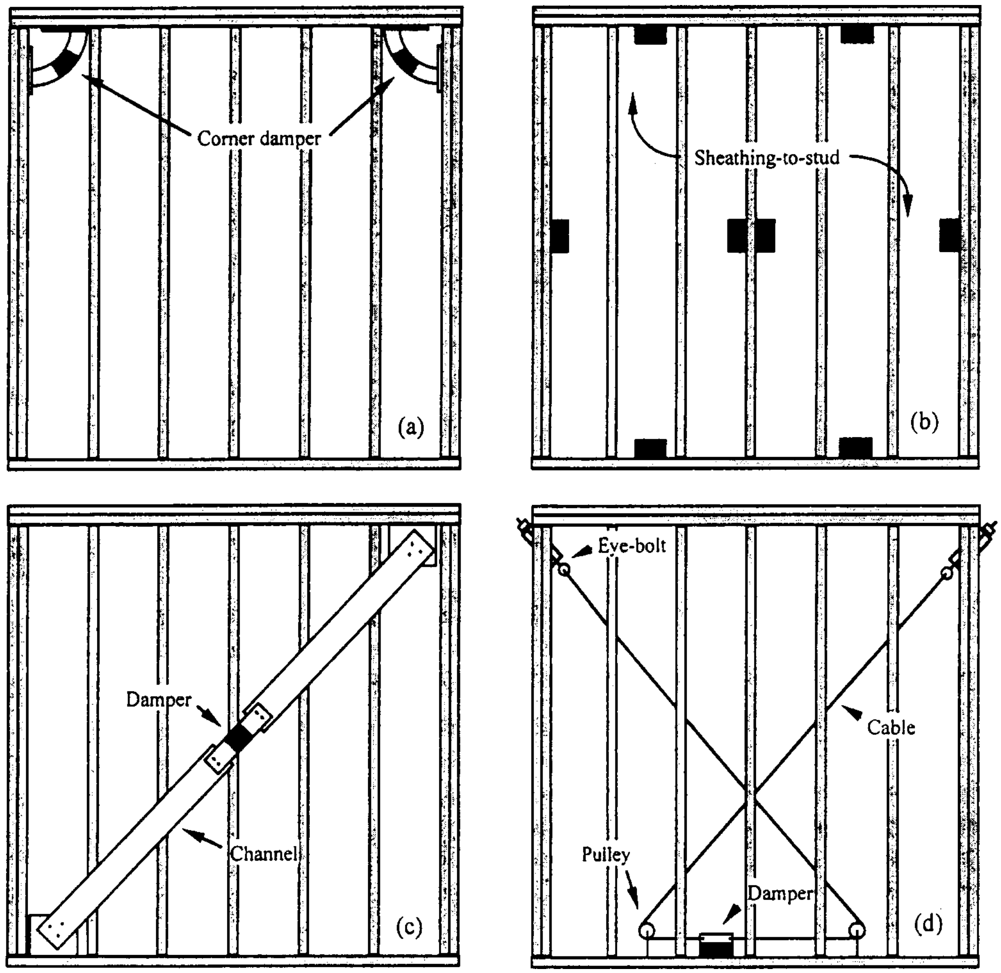

Figure 17. Test configurations for shear wall with viscoelastic dampers. (From Dinehart et al. 1999, © Earthquake Engineering Research Institute. Reproduced with permission.)

displacement corresponding to the ultimate load was approximately 55% larger for the viscoelastically damped wall with the damper along the diagonal as compared to the conventional wall). It should also be understood that the conventional walls must dissipate all of the input energy, primarily via inelastic behavior of the wall. In contrast, for the viscoelastically damped walls a portion of the input energy is dissipated by the viscoelastic dampers and thus the energy dissipation demand on the wall itself may be appreciably reduced.

A comparison of energy dissipation per cycle for three shear wall configurations is shown in Figure 20. The energy dissipation is shown for four cycles of motion at a displacement amplitude equal to the so-called first major event (i.e., ± 1.80 cm). Note that the energy dissipation capacity of both the conventional and viscoelastically damped shear walls decreases as the number of cycles increases. However, the degradation for

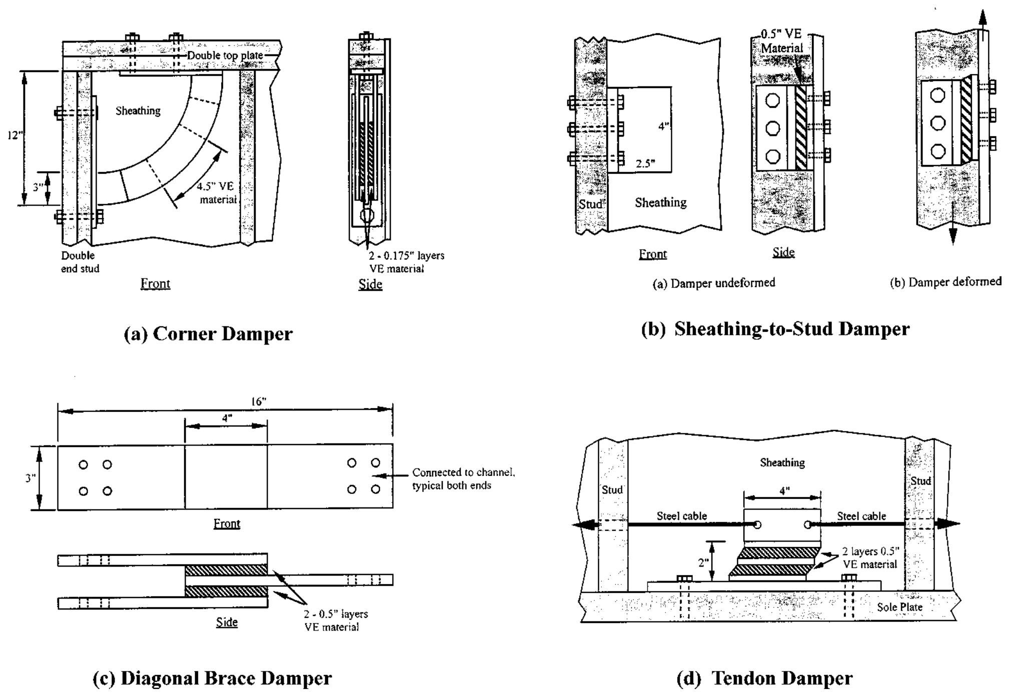

Figure 18. Detailed view of four viscoelastic damper test configurations. (Adapted from Dinehart et al. 1999, © Earthquake Engineering Research Institute. Reproduced with permission.)

both configurations is due to the inelastic behavior of the shear wall (since the reduction in energy dissipation from the one cycle to the next is approximately equal for both configurations). Thus, the viscoelastic dampers provide a stable source of energy dissipation during cyclic motion of the shear wall. A stable source of energy dissipation is particularly important in terms of the ability of a wood-framed structure to resist strong earthquake aftershocks.

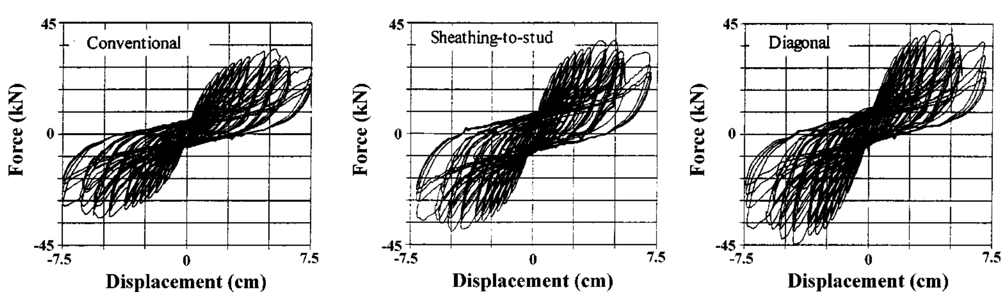

Figure 19. Hysteresis loops for conventional shear wall and viscoelastically damped shear wall. (Adapted from Dinehart et al. 1999, © Earthquake Engineering Research Institute. Reproduced with permission.)

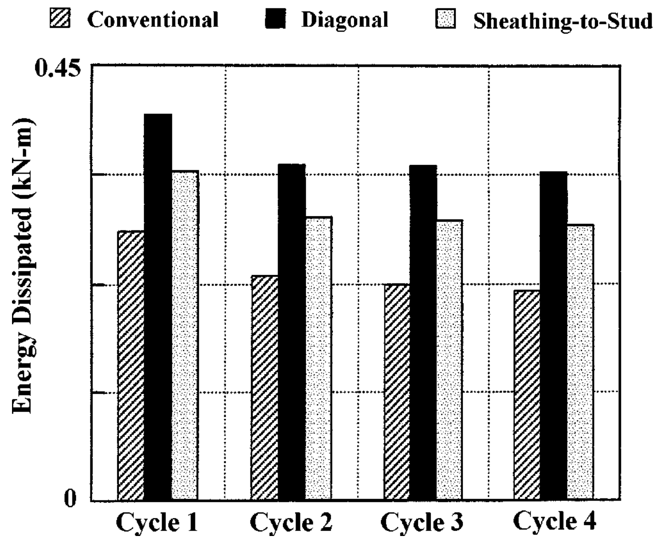

Figure 20. Effect of viscoelastic dampers on energy dissipation of shear walls. (Adapted from Dinehart et al. 1999, © Earthquake Engineering Research Institute. Reproduced with permission.)

HIGGINS (2001)

The application of a hysteretic damper to a wood-framed shear wall is investigated by Higgins (2001). The hysteretic damper consists of a diagonal brace with a fixed anchorage at the top corner of the wall and a sliding anchorage at the opposite corner (see Figure 21). In compression, the diagonal rod is allowed to slip through the sliding anchorage, eliminating the possibility of buckling. In tension, the diagonal rod is gripped by the sliding anchorage. The damper behavior has the apparent effect of expanding the

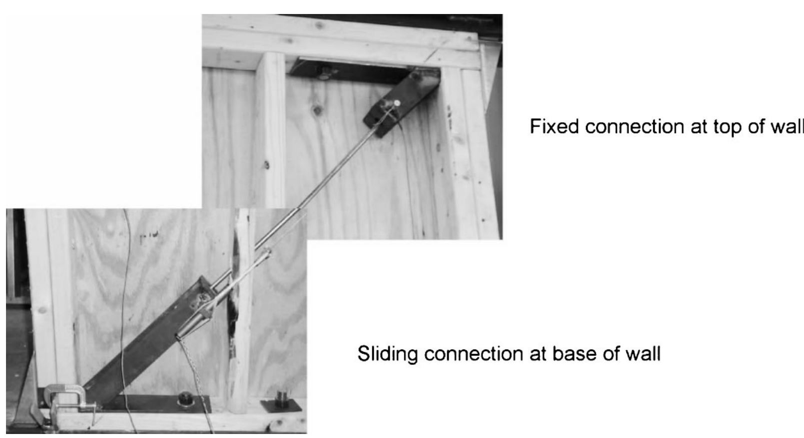

Figure 21. Fixed and sliding anchorage connections for hysteretic damper. (From Higgins 2001, © American Society of Civil Engineers. Reproduced with permission.)

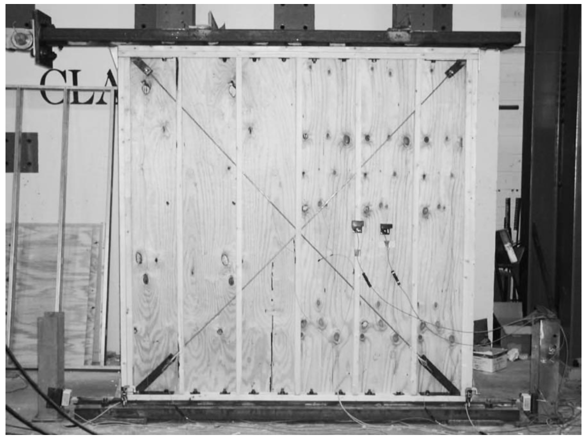

Figure 22. Experimental testing arrangement for wood-framed shear wall with hysteretic dampers along diagonals. (From Higgins 2001, © American Society of Civil Engineers. Reproduced with permission.)

kinematic surface of the element and thus the damper is called a "kinematically expanding hysteretic damper." Note that the term "hysteretic" is used to describe the damper since its behavior is displacement-dependent rather than velocity-dependent.

Experimental tests were performed in which a wood-framed shear wall was outfitted with two of the dampers; one along each diagonal (see Figure 22). The response of the wall with and without the damper when subjected to reversed cyclic loading of increasing displacement amplitude is shown in Figure 23. Figure 23 demonstrates that the dampers were effective in reducing the strength and stiffness degradation of the wall and increasing the energy dissipation capacity. In addition, the characteristic pinching behavior of wood-framed shear walls is virtually absent for the wall with the damper. The dampers eventually failed by fracture on the gross cross section of the diagonal rod.

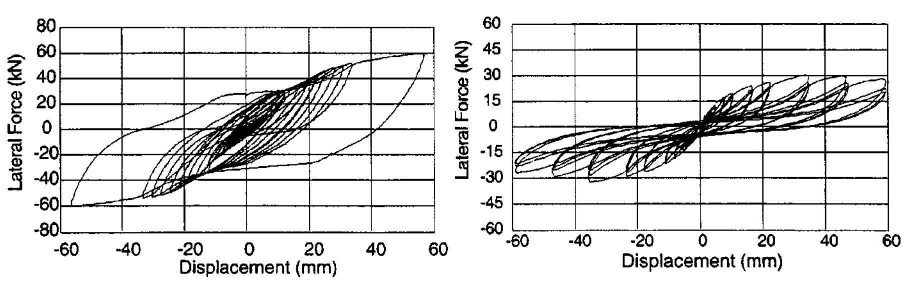

Figure 23. Reversed cyclic loading response of wall with and without hysteretic dampers. (From Higgins 2001, © American Society of Civil Engineers. Reproduced with permission.)

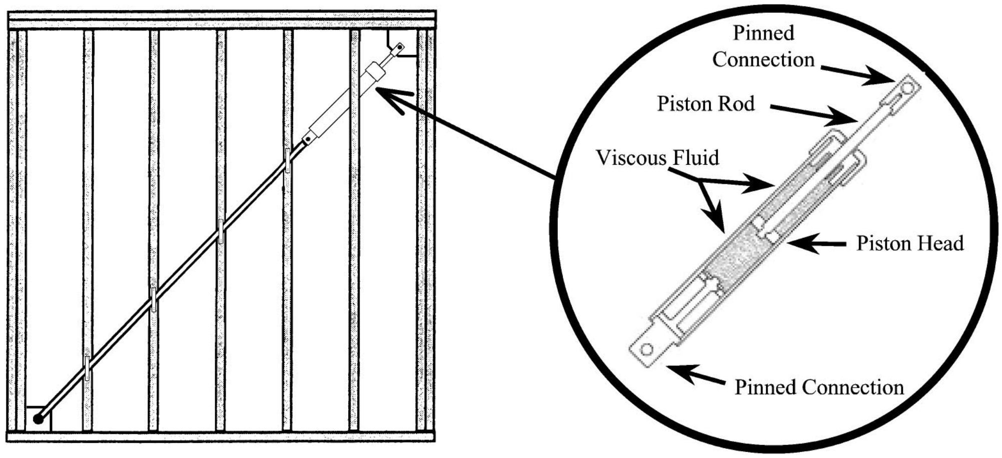

Figure 24. Schematic of fluid viscous damper and orientation within shear wall.

A numerical study is also presented in which a simple structure is subjected to an earthquake record. The study indicates that the proposed damper is more effective in reducing peak displacements than both ordinary tension-only bracing and ADAS/UBB (added damping and stiffness or unbonded brace) devices.

SYMANS et al. (2002)

The seismic response of a wood-framed shear wall with fluid viscous dampers is presented in a numerical study by the authors (Symans et al. 2002). A wall model was developed based on a series of walls that were experimentally tested by Dolan (1989). The weight at the top of the wall was such that the wall represented a single wall in the first story of a three-story apartment building. A nonlinear finite element model of the shear wall was developed and utilized to perform the numerical simulations. The inelastic behavior of the wall was accounted for via nonlinear sheathing connections.

Fluid viscous dampers were oriented within the shear wall framing as shown in Figure 24. The fluid viscous damper, as shown in the exploded view of Figure 24, consists of a cylinder filled with a low-viscosity fluid. As the damper is cycled, the fluid passes through small orifices at high speeds, resulting in the development of heat energy that is transferred to the environment via convection and conduction. For the range of frequencies typical of the fundamental mode of light-framed residential wood construction (say less than about 5 Hz), the fluid damper can be designed to exhibit insignificant restoring force resulting in behavior that is essentially linear viscous (Symans and Constantinou 1998). The design of structures that incorporate such dampers becomes simplified since the dampers may be regarded as simply adding additional energy dissipation capacity to the structure. Of course, one must recognize that the installation of supplemental dampers will alter the load path for the transfer of forces within the structure. Note that, in spite of the relatively low-viscosity of the silicone oil within the damper, such dampers are often referred to as *fluid viscous dampers*, giving the impression that the fluid within

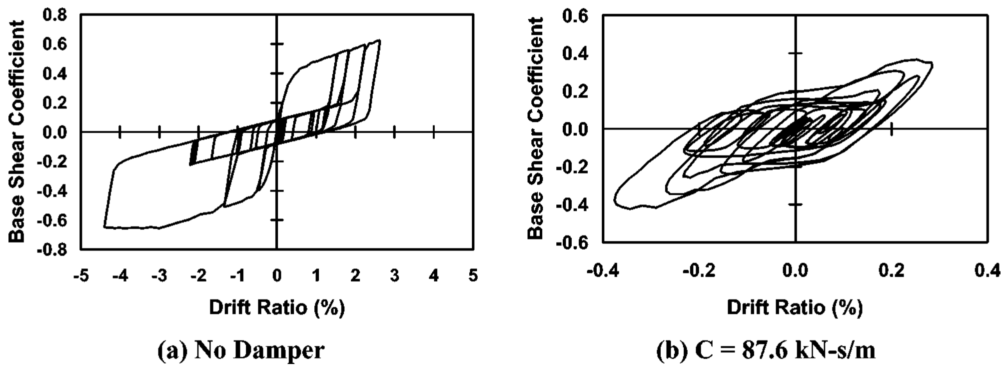

Figure 25. Hysteresis loops of shear wall without and with fluid viscous dampers subjected to Newhall Earthquake Record (*not plotted to same scale*).

the damper is highly viscous. The term fluid viscous damper is the result of the hysteretic behavior of the damper with is equivalent to a linear viscous dashpot.

The authors believe that fluid dampers offer considerable promise for application within wood-framed buildings due to their high-energy dissipation density (i.e., their ability to dissipate large amounts of energy in comparison to their size). The high-energy dissipation density allows the dampers to be conveniently located within the walls of a wood-framed structure. For example, in Figure 24, dual let-in rods are used to connect the lower corner of the wall to one end of the damper. One rod is located on each side of the wall and small metal straps are used to prevent lateral buckling of the rod. One advantage to this configuration is that the damper force lies concentrically within the plane of the wall and thus there are no bending moments applied to the wall at the corner connections. Furthermore, this configuration maintains a certain level of gravity load carrying capacity and does not interfere with the installation of sheathing on either side of the wall. However, a disadvantage to this configuration is that the effectiveness of the damper is reduced by 50% due to the diagonal orientation. Alternate damper configurations in which the vertical studs are rotated 90° are currently under development. In addition, it is envisioned that the wall segments that contain fluid viscous dampers would be prefabricated units that would simply be "dropped-in" during construction. Note that, to the authors' knowledge, there has been only one application of fluid viscous dampers to a wood structure. The structure is a commercial timber-framed building in Alaska that was seismically retrofitted in 1997 using two fluid viscous dampers (force capacity =445 kN; stroke=±64 mm) within diagonal bracing.

The seismic response of the wall was evaluated for two historical earthquake records, one a far-field motion and the other a near-field motion. Selected results for the near-field motion (Newhall record [90° component] of the 1994 Northridge Earthquake) are presented herein. The wall was outfitted with a damper having a viscous damping coefficient of 87.6 kN-s/cm, resulting in an increase in the fundamental mode-damping ratio from an assumed value of 2% (under elastic conditions) for the wall without a damper to a value of approximately 20%. The effectiveness of the damper is clearly depicted in Figure 25. Note that the two hysteresis loops are not plotted to the same scale on the

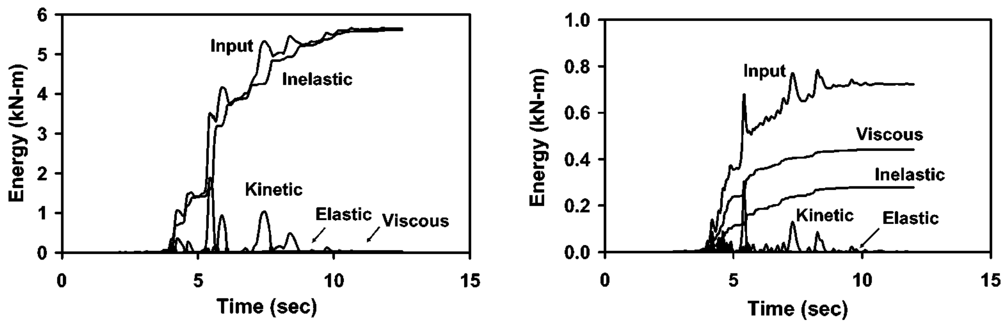

(a) No Damper **(b) C = 87.6 kN-s/m**

Figure 26. Energy distribution within wall for Newhall Earthquake Record: (a) no damper and (b) with fluid viscous damper.

horizontal axis. For the wall without a damper, the hysteresis loop of Figure 25a clearly demonstrates the strongly nonlinear behavior of the wall for this near-field earthquake record. The potential for damage to the wall can be conveniently characterized by the drift ratio. According to the *NEHRP Guidelines for the Seismic Rehabilitation of Buildings* (ATC 1997), for light-framed wood construction, the transient drift ratios corresponding to the structural performance levels of Immediate Occupancy (IO), Life-Safety (LS), and Collapse Prevention (CP) are 1%, 2% and 3%, respectively. For the wall alone (i.e., no damper), the drift ratio in the wall exceeds 3% and thus is regarded as having failed. For the wall with the damper (see Figure 25b), the peak drift was reduced to 0.37 % (a reduction of 88% from the failure drift ratio of 3%). Thus, the dampers are effective in preventing failure and minimizing damage to the wall. The peak damper force, velocity, and stroke are 8.66 kN, 9.88 cm/s, and 5.99 mm, respectively. A damper with such behavior can be readily manufactured. Furthermore, one may note the larger forces that develop within the small displacement region of the pinching zone for the case of the wall with the damper. This is the result of the damper force being velocity-dependent, thus leading to large damper forces in the region of the pinching zone where the displacements are small and the velocities are large. The development of larger forces in the pinching region is one of the reasons that the dampers are so effective.

The performance of the fluid dampers may also be evaluated by considering the energy distribution within the wall during the earthquake. The time histories of various energy quantities are shown in Figure 26 for the wall with and without the fluid damper. Note that the two plots shown are plotted at different scales on the vertical axis. Figure 26a indicates that, without a fluid damper, essentially all of the seismic input energy is eventually dissipated via inelastic behavior in the wall. In contrast, Figure 26b demonstrates a significant reduction in energy dissipation demand on the wall (reduction of approximately 95% compared to no damper case) while the viscous energy dissipated by the fluid damper represents a large portion of the final seismic input energy (approximately 57%). Thus, the fluid damper has effectively provided for a transfer of energy dissipation demand from the wall to the damper. One may also note that the seismic input energy is not the same for the wall with and without the damper. This is the case since the input energy was defined as the integral of the base shear over the ground displacement. Since the base shear is different for the wall with and without the damper, the input energy is also different.

SUMMARY

Although there has been a steadily increasing growth in the application of advanced seismic protection systems within concrete and steel structures, the application within wood structures is essentially stagnant. This is in spite of the fact that light-framed wood structures experienced extensive damage during the 1994 Northridge Earthquake. Of course, there are a number of impediments to the implementation of base isolation and supplemental damping systems in wood-framed structures. For example, the application of a base isolation system to a wood-framed structure would require the introduction of a stiff diaphragm at the first floor and the introduction of flexible utility connections while the application of a supplemental damping system would require a modified framing arrangement. In spite of the impediments to implementation, it is evident from the literature reviewed in this paper that advanced seismic protection systems in the form of base isolation systems and supplemental damping systems offer promise for improving the performance of wood structures subjected to strong seismic loading.

ACKNOWLEDGMENTS

This research was carried out under contract to Consortium of Universities for Research in Earthquake Engineering (CUREE) as part of the CUREE-Caltech Woodframe Project ("Earthquake Hazard Mitigation of Woodframe Construction"), under a grant administered by the California Office of Emergency Services and funded by the Federal Emergency Management Agency (FEMA). The author is solely responsible for the information contained herein. No liability for the information contained herein is assumed by Consortium of Universities for Research in Earthquake Engineering, California Institute of Technology, California Office of Emergency Services, or the Federal Emergency Management Agency.

REFERENCES

Applied Technology Council (ATC), 1997. *NEHRP Guidelines for the Seismic Rehabilitation of Buildings, FEMA 273 (ATC 33)*, prepared for the Building Seismic Safety Council, published by the Federal Emergency Management Agency, Washington DC.

Constantinou, M. C., Soong, T. T., and Dargush, G. F., 1998. *Passive Energy Dissipation Systems for Structural Design and Retrofit*, MCEER Monograph No. 1, Multidisciplinary Center for Earthquake Engineering Research, Buffalo, NY.

Constantinou, M. C., and Symans, M. D., 1993a. Seismic response of buildings with supplemental damping, *Struct. Des. Tall Build.* **2**, 77–92.

Constantinou, M. C., and Symans, M. D., 1993b. Experimental study of seismic response of buildings with supplemental fluid dampers, *Struct. Des. Tall Build.* **2**, 93–132.

Delfosse, G. C., 1982. Wood framed individual houses on seismic isolators, *Proc. of the International Conf. on Natural Rubber for Earthquake Protection of Buildings and Vibration Isolation*, Kuala Lumpur, Malaysia, February, pp. 104–111.

Dinehart, D. W., and Shenton, H. W., 1998. Comparison of the response of timber shear walls with and without passive dampers, *Proc. of Structural Engineers World Congress*, San Francisco, CA, July, Paper T207-5.

Dinehart, D. W., Shenton, H. W., and Elliott, T. E., 1999. The dynamic response of wood-frame shear walls with viscoelastic dampers, *Earthquake Spectra* **15** (1), 67–86.

Dolan, J. D., 1989. The dynamic response of timber shear walls, Ph.D. dissertation, University of British Columbia, Dept. of Civil Engineering, Vancouver, B.C., Canada.

Filiatrault, A., 1990. Analytical predictions of the seismic response of friction damped timber shear walls, *Earthquake Eng. Struct. Dyn.* **19**, 259–273.

Higgins, C., 2001. Hysteretic dampers for wood frame shear walls, *Proc. of the 2001 Structures Congress and Exposition*, ASCE, edited by P. C. Chang, Washington, DC, May.

Kircher, C., Reitherman, R., Whitman, R., and Arnold, C., 1997. Estimation of earthquake losses to buildings, *Earthquake Spectra* **13** (4), 703–720.

Pall, A. S., and Pall, R., 1991. Seismic response of a friction-base-isolated house in Montreal, *Proc. of Sixth Canadian Conf. on Earthquake Engineering*, Toronto, Canada, June, pp. 375–382.

Reed, J. W., and Kircher, C. A., 1986. Base isolation of a five-story wood-frame building, *Proc. of a Seminar and Workshop on Base Isolation and Passive Energy Dissipation (ATC-17)*, San Francisco, CA, March, pp. 133–142.

Sakamoto, I., Ohashi, Y., and Fujii, Y., 1990. Seismic behavior of base isolated two-storied wooden building, *Proc. of the 1990 International Timber Engineering Conf.*, Tokyo, Japan, **3**, pp. 938–945.

Soong, T. T., and Constantinou, M. C. (editors), 1995. *Passive and Active Structural Vibration Control in Civil Engineering*, Springer-Verlag, New York.

Symans, M. D., Cofer, W. F., Fridley, K. J., and Du, Y., 2002. Effects of supplemental energy dissipation systems on the seismic response of light-framed wood buildings, *Proc. of Seventh National Conf. on Earthquake Engineering*, Boston, MA, July.

Symans, M. D., and Constantinou, M. C., 1998. Passive fluid viscous damping systems for seismic energy dissipation, *J. of Earthquake Technology, ISET, Special issue on passive control of structures,* **35** (4), 185–206.

Zayas, V. A., and Low, S. S., 1997. Seismic isolation of a four-story wood building, *Earthquake Performance and Safety of Timber Structures*, Forest Products Society, Proc. No. 7289, pp. 83–91.

(Received 22 March 2000; accepted 27 April 2002)